Oncogenic role of the TP53-induced glycolysis and apoptosis regulator in nasopharyngeal carcinoma through NF-κB pathway modulation

MING ZHAO*, JUAN FAN*, YONG LIU, YANXIN YU, JINHUI XU, QINGLIAN WEN, JIANWEN ZHANG, SHAOZHI FU, BIQIONG WANG, LI XIANG, JING FENG, JINGBO WU and LINGLIN YANG

Department of Oncology, The First Hospital of Sichuan Medical University, Luzhou, Sichuan 646000, P.R. China

Received October 16, 2015; Accepted December 2, 2015

DOI: 10.3892/ijo.2015.3297

Abstract. The TP53-induced glycolysis and apoptosis regulator (TIGAR) is a p53 target gene, which functions to suppress reactive oxygen species (ROS) damage and protect cells from apoptosis. In this study, we investigated the role of TIGAR in nasopharyngeal carcinoma (NPC) tumorigenesis. Imnunohistochemical analysis of the tissue specimens from nasopharyngeal carcinoma patients showed a higher expression level of TIGAR in tumor tissues, compared with normal nasopharyngeal epithelium. Knockdown of TIGAR by lentivirus-shRNA in CNE-2 or 5-8F cells resulted in decreased cell growth, colony formation, migration, invasion, and induced apoptosis. TIGAR overexpression exerted the opposite effects except for apoptosis reduction. In the xenograft tumor models, TIGAR knockdown reduced tumor growth rate and weight, whereas TIGAR overexpression showed the opposite effects. In addition, the NF-κB signaling pathway was decreased in TIGAR silenced cells. In conclusion, our data demonstrated that TIGAR acted as an oncogene in NPC tumorigenesis, and knockdown of TIGAR inhibited NPC tumor growth through the NF-κB pathway.

Introduction

Nasopharyngeal carcinoma (NPC) is a squamous cell carcinoma extremely common in southern regions of China and Southeast Asia, characterized by a local invasion or early distant metastasis at the time of diagnosis (1). Although it is radiosensitive (2), a high number of patients show local regional recurrence or metastatic spread (3). Therefore, it is of utmost importance to understand the pathogenic mechanism of NPC for an early diagnosis to apply effective therapeutic strategies.

TIGAR was first identified as a P53 target gene, playing an important role in glycolysis and apoptosis in U2OS cells (4). It represents a key gene in the metabolism control mediated by P53 (5). Due to the enzymatic activity of the encoded protein, TIGAR reduces fructose-2,6-bisphosphate (F-2,6-P2) levels, leading to glycolysis inhibition and pentose phosphate pathway (PPP) induction (4). In addition, the PPP enhances the production of nicotinamide adenine dinucleotide phosphate (NADPH), which scavenges intracellular reactive oxygen species (ROS) and protects cells from oxidative stress-induced apoptosis (4).

An increasing number of studies reported that TIGAR modified expression is tightly correlated with cancer development. A high expression level of TIGAR was observed in cancers such as invasive breast cancer (6), hepatocellular carcinoma (7), intestinal cancer (8), and glioblastoma (9,10). TIGAR protects cancer cells from apoptosis in breast cancer and hepatocellular carcinoma (6,7). In a mouse intestinal cancer model, transgenic mouse knockout for the TIGAR gene showed a reduced tumor burden and an increased survival (8). Knockdown of TIGAR in glioma cells can enhance radiosensitivity by ROS accumulation, which results in DNA damage and cellular senescence (11). These studies suggested that TIGAR may act as an oncogene in some cancers to support cancer progression.

However, the exact role of TIGAR in NPC has not been yet reported. The present study aimed to investigate the role of TIGAR in NPC tumorigenesis. Our results showed a high expression of TIGAR in the tumor tissue of NPC patients compared with the expression in the adjacent normal epithelium. Knockdown of TIGAR in NPC cells reduced tumor growth and increased apoptosis via NF-κB pathway. On the other hand, TIGAR overexpression promoted tumor growth, although did not decrease apoptosis. These data strongly suggested that TIGAR might represent an important oncogene in NPC tumorigenesis.

Materials and methods

Clinical samples. A total of 96 NPC patients were selected at The First Hospital of Sichuan Medical University, Luzhou,

Correspondence to: Professor Jingbo Wu or Professor Linglin Yang, Department of Oncology, The First Hospital of Sichuan Medical University, 25 Taiping Street, Luzhou, Sichuan 646000, P.R. China
E-mail: wjb6147@163.com
E-mail: yanglluyi@126.com

*Contributed equally

Abbreviations: TIGAR, TP53-induced glycolysis and apoptosis regulator; NPC, nasopharyngeal carcinoma; NF-κB, nuclear factor κB; Lenti-shRNA, lentivirus-mediated small hairpin RNA; MMP-2, matrix metalloproteinase-2; MMP-9, matrix metalloproteinase-9

Key words: TP53-induced glycolysis and apoptosis regulator, nasopharyngeal carcinoma, xenograft model, NF-κB pathway

China. Written informed consent was obtained from the patients, and this program was approved by the Ethics Committee of the First Hospital of Sichuan Medical University.

Immunohistochemical staining. The tissue specimens from the patients were immunostained with a rabbit polyclonal TIGAR antibody (1:200, Santa Cruz Biotechnology, Santa Cruz, CA, USA), according to the manufacturer's instructions. Two pathologists independently scored each slide. The percentage of positive tumor cells was evaluated (0, 0%; 1, 1-25%; 2, 26-50%; 3, 51-75%; 4, 76-100%), as well as the staining intensity (0, negative; 1, weak; 2, moderate; 3, strong; 4, very strong), as previously described (12). The intensity score x percentage score value was used to obtain the final overall score for TIGAR (0-16).

Cell culture. The human normal nasopharyngeal epithelial cell line NP69-SV40T (Sun Yat-sen University Cancer Center, Guangdong, China), was routinely maintained in keratinocyte serum-free medium supplemented with human recombinant epidermal growth factor (EGF 1-53) and bovine pituitary extract (BPE) (Invitrogen, USA). The human CNE-2 and 5-8F NPC cell lines were obtained from ATCC (American Type Culture Collection), and routinely maintained in RPMI-1640 medium supplemented with 10% fetal bovine serum (GE Healthcare Life Sciences, Logan, UT, USA), 100 U/ml penicillin, and 100 μg/ml streptomycin (Beyotime Biotecnology, China).

Lentivirus-mediated small hairpin RNA (Lenti-shRNA) against TIGAR. The Lenti-shRNA vector system against TIGAR was constructed, packed, and purified by GeneChem (Shanghai, China). The shRNA oligonucleotides were designed as TIGAR-shRNA (GCCAGCTTTACTGGAGAACTT). A scramble sequence was synthesized as control, and tagged as Scramble-shRNA (TTACCGAGACCGTACGTAT). Human NPC cells CNE-2 and 5-8F were infected, and colonies expressing a stable shRNA were selected using puromycin (Sigma-Aldrich, St. Louis, MO, USA), according to the manufacturer's protocol.

Cell growth assay and colony formation assay. For cell growth assay, stable cells were seeded at a density of $5x10^4$ per well. The cells were stained by trypan blue and counted in the following 5 days. For colony formation assay, stable cell lines transfected with TIGAR-shRNA and Scramble-shRNA were seeded in 3.5-mm culture dishes at a density of 200. The colony formation was evaluated under the microscope after 10 days. Next, the cells were fixed with 4% PFA, and stained with 0.1% crystal violet. Data are expressed as the mean ± SD of five independent experiments.

EdU assay. Stable cells were seeded on coverslips in 24-well plate at a density of $2x10^4$ per well. Twenty-four hours later, cells were incubated with EdU (20 μM) for 1.5 h. Then, EdU assay were continued using EdU DNA Proliferation *In Vitro* Detection kit (RiboBio Co., Ltd., Guangzhou, China), according to the manufacturer's instructions. In total, three fields per slice were randomly selected and analyzed, and experiment was repeated three times. The EdU incorporation rate was calculated as the ratio of the EdU positive cell number to the total cell number in each feld.

Wound healing assay and Transwell migration assay. Cells at 80-90% confluence were scraped using a sterile micropipette tip across the monolayer to obtain a longitudinal scratch without cells, to perform the wound healing assay. The empty area was monitored every 4 h. The Transwell assay was performed using Transwell chambers with polycarbonate filters (8-μm pore size, BD Biosciences, San Jose, CA, USA). The chambers were coated with 50 μl Matrigel prior to cell seeding, and immersed in a well containing 600 μl of complete medium, followed by the addition of $4x10^4$ cells in 100 μl serum-free medium to the upper chamber. After an incubation of 24-48 h at 37˚C in a 5% CO_2 incubator, cells were fixed with 4% PFA, and stained with 0.1% crystal violet. The cells remained in the upper chamber were removed with a cotton swab. The migrated cells were counted under a microscope at x400 magnification.

Apoptosis analysis. Stable cell lines were harvested at 48 h after adriamycin (0.5 μg/ml) stimulation, and stained for Annexin V-FITC and PI at room temperature for 15 min according to the manufacturer's instructions (Invitrogen). Cells were analyzed by flow cytometry (FACScan, Becton-Dickinson).

Xenograft tumor induction. Eight-week-old male nude mice (BALB/c-nu) were bought from Beijing HFK Bioscience Co. Ltd., Beijing, China. The cells expressing TIGAR-shRNA or Scramble-shRNA were collected and resuspended in PBS at the density of 10^7/ml, and 100 μl (10^6 cells) were subcutaneously inoculated in the flank of each mouse. Tumor volumes were monitored every 3 days and the length, width and height were measured to evaluate the tumor volume through the following formula: Tumor volume (mm^3) = 0.5 x length x width x height (13). After the designated days, mice were sacrificed by carbon dioxide asphyxiation, and the tumors were removed for analysis. The animal experiments were approved by the Ethics Committee of Luzhou Medical College, Luzhou, China.

Western blot analysis. Total cell proteins were extracted with RIPA lysis buffer with cocktail of protease inhibitors (Beyotime Biotecnology). The samples were resolved on a SDS-PAGE gel and then transferred to a PVDF membrane (Amersham Biosciences, Fairfield, CT, USA). The membranes were labeled with the following antibodies of the proteins of interest: TIGAR (sc-166290; Santa Cruz Biotechnology); Caspase-3 (19677-1-AP; Proteintech, Wuhan, China); p65 (AN365, Beyotime Biotecnology); IkB-α (AI096, Beyotime Biotecnology); Bcl-2 (12789-1-AP, Proteintech); MMP-2 (10373-2-AP, Proteintech); MMP-9 (10375-2-AP, Proteintech); Oct-1 (10387-1-AP, Proteintech); GAPDH (2118; Cell Signaling, Beverly, MA, USA). Secondary antibodies were purchased from Proteintech. ECL was used (Amersham Biosciences) for the detection of the target bands.

Statistical analysis. The experiments were performed at least in triplicate. The results were expressed as the mean ± SD.

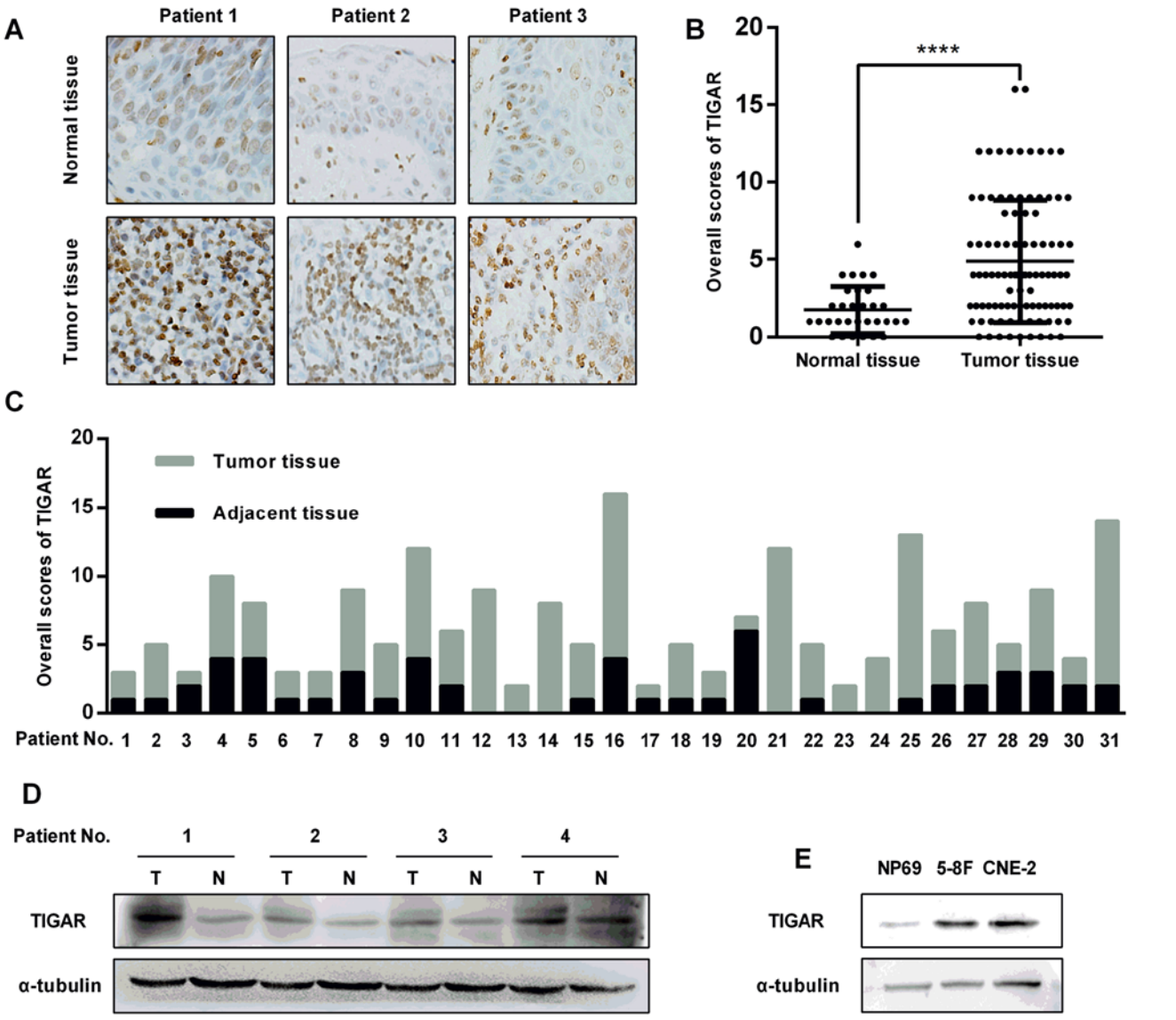

Figure 1. TIGAR is overexpressed in human NPC. (A) TIGAR showed higher expression in NPC tumor tissue (lower panel) compared with the adjacent normal epithelium (upper panel). The original magnification was x400. (B) The NPC tumor tissues showed significantly elevated overall scores of TIGAR compared with the normal nasopharyngeal epithelium. (C) The elevated overall scores of TIGAR are displayed in the NPC tissues compared with the corresponding nasopharyngeal epithelium. (D) Western blot analysis confirmed the overexpression of TIGAR in representative NPC tumor tissues (T) as well as the lack of TIGAR in the adjacent normal epithelium (N). (E) Western blot analysis showed higher expression of TIGAR in NPC cell lines (5-8F, CNE-2) compared to the normal nasopharyngeal epithelial cells (NP69). The results were expressed as the mean ± SD. ****P<0.0001.

Statistical analysis was performed by SPSS software and GraphPad Prism. P<0.05 was considered statistically significant.

Results

Enhanced expression of TIGAR in NPC. TIGAR expression was evaluated in NPC tissue specimens by immunohistochemistry (IHC). TIGAR staining intensity in NPC cells was significantly stronger compared to the staining in the adjacent normal epithelial cells (Fig. 1A). Next, the immunostaining of the 96 slides from the NPC patients was scored, showing a higher overall score in the tumor tissues compared with the normal nasopharyngeal epithelium (Fig. 1B). Among these slides, 31 specimens with both the NPC tissues and the adjacent normal epithelium were selected, showing a similar result as that shown in Fig. 1B (Fig. 1C). The remarkably elevated protein level in primary NPC tissues was confirmed using immunoblotting (Fig. 1D). A similar result was also observed in NPC cells (CNE-2, 5-8F) and normal nasopharyngeal epithelial cells (NP69) (Fig. 1E).

Knockdown of TIGAR suppresses proliferation, migration, invasion, and colony formation on NPC cells. To explore the biological function of TIGAR in NPC cells, lentivirus was used to introduce shRNA (Lenti-shRNA) targeting TIGAR into CNE-2 and 5-8F cells (Fig. 2). The western blot analysis showed a remarkable reduction of TIGAR level in TIGAR-shRNA cells compared with TIGAR expression in Scramble-shRNA cells (Fig. 2A). ROS accumulation and GSH/GSSG reduction also confirmed the high depletion efficiency of TIGAR (data not shown). Cell growth assays revealed a

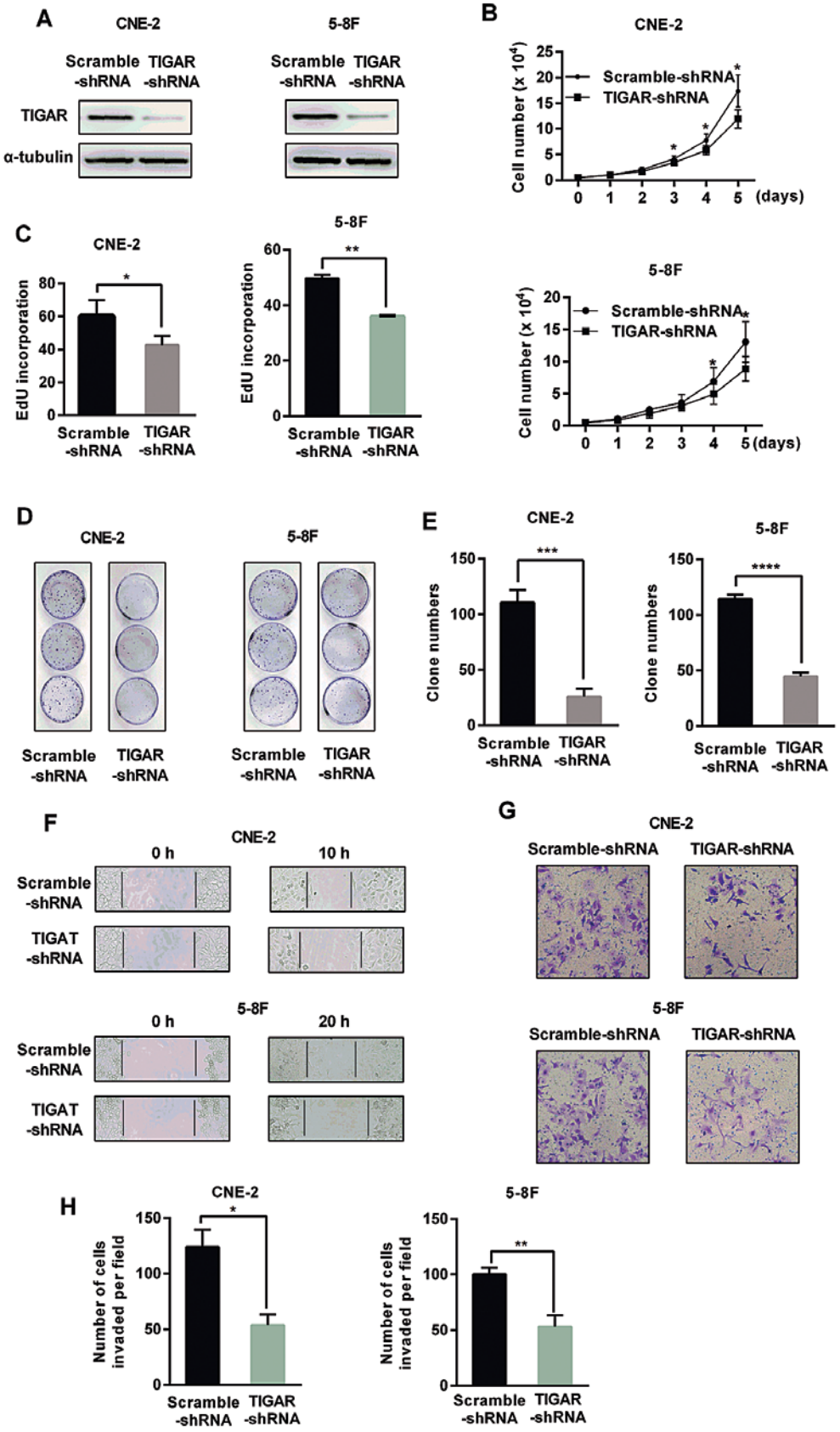

Figure 2. Knockdown of TIGAR supresses proliferation, colony formation, migration and invasion in human NPC cells. (A) Western blot analysis of TIGAR levels in stable cells. (B) Cell growth was monitored by trypan blue exclusion assay. (C) Cell proliferation rate was evaluated by EdU incorporation. (D) Representative images of colony formation. A number of 200 cells were seeded in a 3.5-mm plate, and incubated for 10 days. (E) The number of colonies was counted and statistically analyzed. (F) Representative images of wound healing assay. The original magnification was x100. (G) Representative images of Transwell assay. Cells were seeded at the number of $4x10^4$, and migrated cells were counted in 4 representative fields after 20 h. The original magnification was x100. (H) Statistically analysis of invaded cells in the Transwell invasion assays. The results were expressed as the mean ± SD from at least three experiments. $^{*}P<0.05$; $^{**}P<0.01$;$^{***}P<0.001$; $^{****}P<0.0001$.

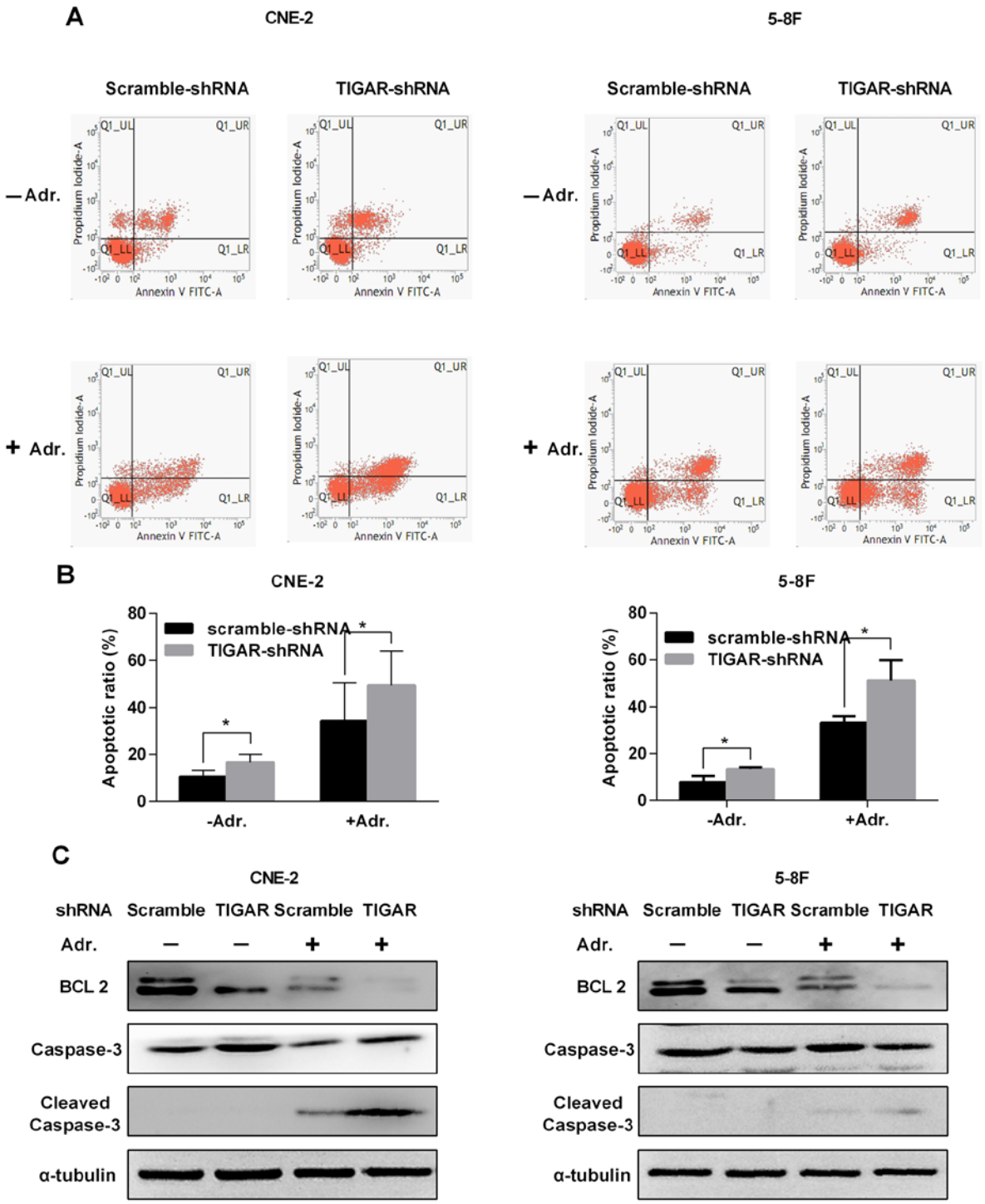

Figure 3. Knockdown of TIGAR induces apoptosis in human NPC cells. (A) Cell apoptosis was evaluated by Annexin V/PI staining and flow cytometry analysis. Adriamycin (0.5 μg/ml) was added and apoptosis was measured after 48 h. (B) Apoptotic rate in adriamycin-treated cells. (C) Protein levels of the anti-apoptotic protein Bcl-2 and caspase-3 were analyzed by western blot analysis. The results were expressed as the mean ± SD from at least three experiments. *P<0.05.

reduced growth in TIGAR-shRNA cells compared to the growth of the Scramble-shRNA cells (Fig. 2B). EdU incorporation confirmed the remarkable reduction of the proliferation in the TIGAR-shRNA cells (Fig. 2C). The number of colonies in TIGAR-shRNA cells was apparently lower than the number in the Scramble-shRNA cells (Fig. 2D and E). In order to investigate whether TIGAR was involved in migration, wound healing assay and Transwell migration assay were performed, showing a significant decreased migration ability in TIGAR-shRNA cells (Fig. 2F and G) as well as a reduced invasion ability, as shown by Matrigel invasion assay (Fig. 2H).

Knockdown of TIGAR induces apoptosis in human NPC cells. To evaluate whether TIGAR depletion affected apoptosis in NPC cells, stable NPC cells were stained with Annexin V/PI and analyzed by flow cytometry (Fig. 3). The results indicated

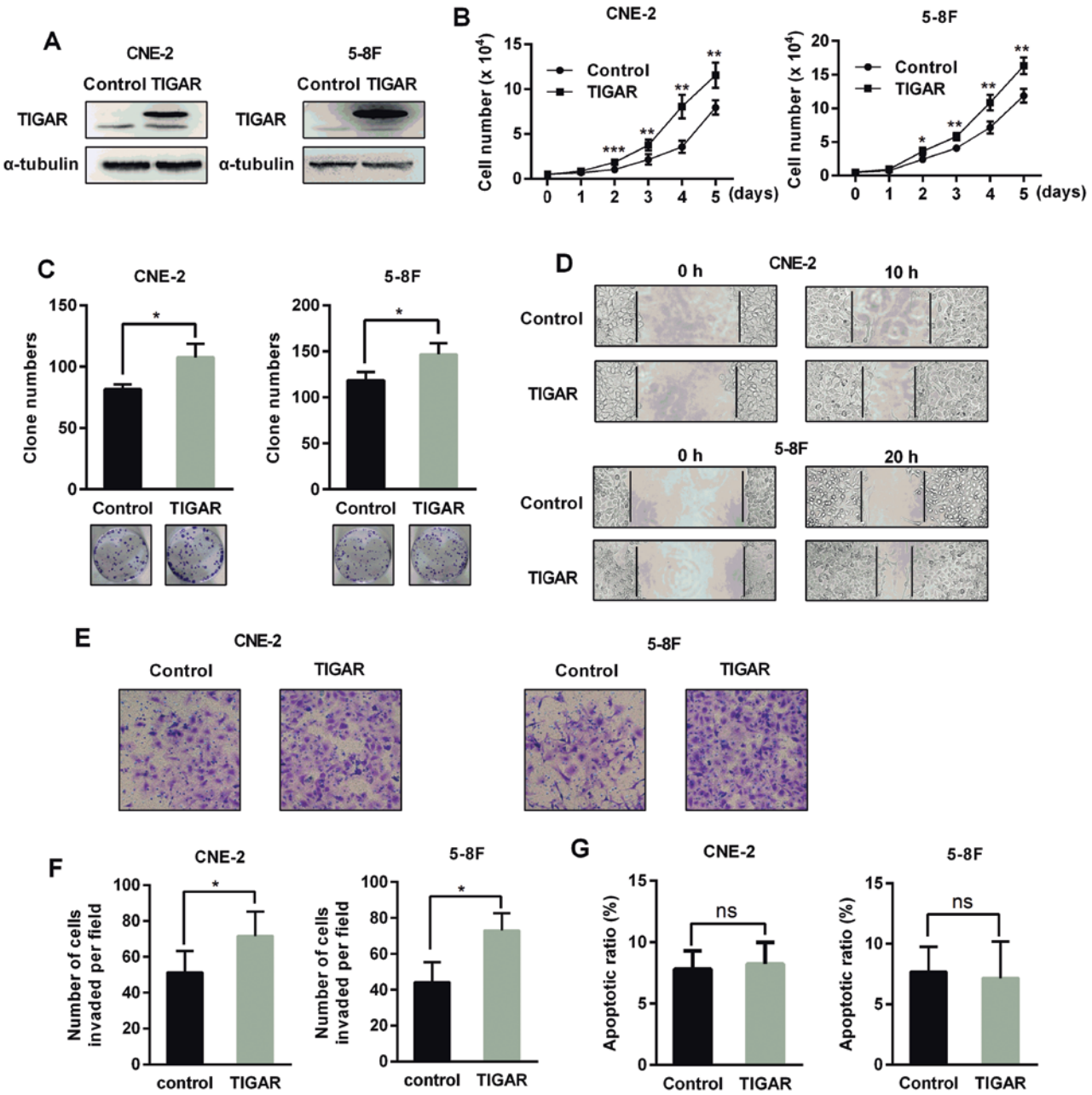

Figure 4. TIGAR overexpression can promote the proliferation, colony formation, migration and invasion in human NPC cells, without reducing apoptosis. (A) Western blot analysis of TIGAR levels in stable cells. (B) Cell growth was monitored by trypan blue exclusion assay. (C) Representative images and statistically analysis of colony formation. (D) Representative images of wound healing assay. The original magnification was x100. (E) Representative images of Transwell assay. The original magnification was x100. (F) Statistically analysis of invaded cells in Transwell invasion assays. (G) Representative images of apoptosis. The results are expressed as the mean ± SD from at least three experiments. *P<0.05; **P<0.01; ***P<0.001.

that the apoptotic rate was increased in TIGAR-shRNA cells compared to the rate in the Scramble-shRNA cells (Fig. 3A and B). To test whether TIGAR depletion can improve the adriamycin related apoptosis, cells were incubated with 0.5 μg/ml adriamycin for 48 h, and analyzed by flow cytometry. As shown in Fig. 3A and B, cell apoptosis was remarkably induced in TIGAR-shRNA cells compared with apoptosis in the Scramble-shRNA cells. We further examined the anti-apoptotic protein BCL2, which was downregulated as we expected, while cleaved caspase-3 was upregulated (Fig. 3C).

TIGAR overexpression promotes proliferation, colony formation, migration and invasion without reducing apoptosis in human NPC cells. To evaluate the effect of TIGAR overexpression on NPC cells, we constructed stable cells overexpressing TIGAR (Fig. 4A). These cells exhibited an increased growth rate, colony formation, and enhanced migration and invasion (Fig. 4B-F). However, TIGAR overexpression did not reduce apoptosis (Fig. 4G).

TIGAR increases NPC xenograft tumor growth. To evaluate whether knockdown of TIGAR reduced tumor growth *in vivo*, NPC stable cells were subcutaneously inoculated into the flank of nude mice. As shown in Fig. 5, the tumor growth rate was decreased in TIGAR-shRNA group compared with the corresponding Scramble-shRNA group. In addition, the tumor

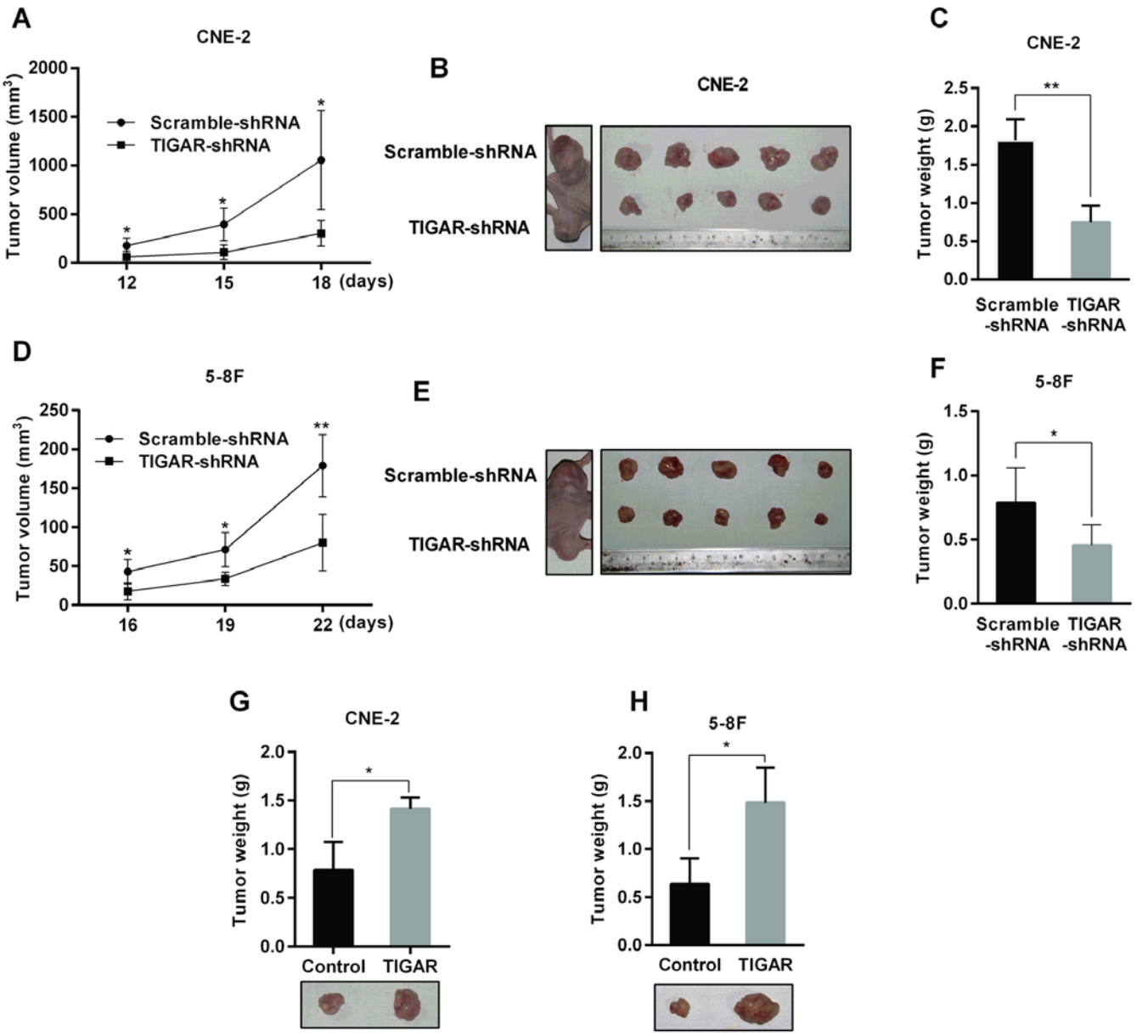

Figure 5. TIGAR accelerates NPC xenograft tumor growth. (A and D) The tumor volume was monitored every three days. (B and E) Representative images of tumors derived from TIGAR-shRNA cells and Scramble-shRNA cells. (C and F) Tumor weight was quantified. (G and H) Cells overexpressing TIGAR were evaluated for NPC xenograft tumor growth. The results were expressed as the mean ± SD. *P<0.05; **P<0.01.

weight in the TIGAR-shRNA group was one-half of the tumor weight in the Scramble-shRNA group (Fig. 5C and F). On the contrary, TIGAR overexpression accelerated xenograft tumor growth in nude mice (Fig. 5G and H).

Knockdown of TIGAR inhibits the NF-κB signaling pathway. The IκB-α and p65 were analyzed to evaluate whether NF-κB pathway was involved in TIGAR-regulated apoptosis in NPC cells. Our results showed increased expression of IκB-α, and inhibited translocation of p65 into the nucleus in both CEN-2 and 5-8F TIGAR-shRNA cells, indicating an inhibited NF-κB pathway (Fig. 6A and B). Immunofluorescence staining of p65 confirmed the reduced level of p65 in the nucleus (Fig. 6C). Next, NF-κB target genes matrix metalloproteinase- 2 (MMP-2) and MMP-9 were examed for a significant reduction in TIGAR-shRNA cells (Fig. 6B).

Discussion

Our results showed that the expression of TIGAR was upregulated in NPC tumor tissues compared with the adjacent normal epithelium. Knockdown of TIGAR in NPC cells CNE-2 or 5-8F and xenograft tumor models indicated a reduced tumor progression and enhanced apoptosis. These results suggest that TIGAR may act as an oncogene in NPC tumorigenesis. Recently, Cheung *et al* reported an increased TIGAR expression in primary human colon cancer, and showed that TIGAR was required for intestinal tumorigenesis (8). Our current results are consistent with these already published results.

As a glycolysis regulator, TIGAR degrades intracellular fructose-2,6-bisphosphate (F-2,6-P2), which resulted in a shift from glycolysis to the pentose phosphate pathway (PPP). On the other hand, knockdown of TIGAR results in increased

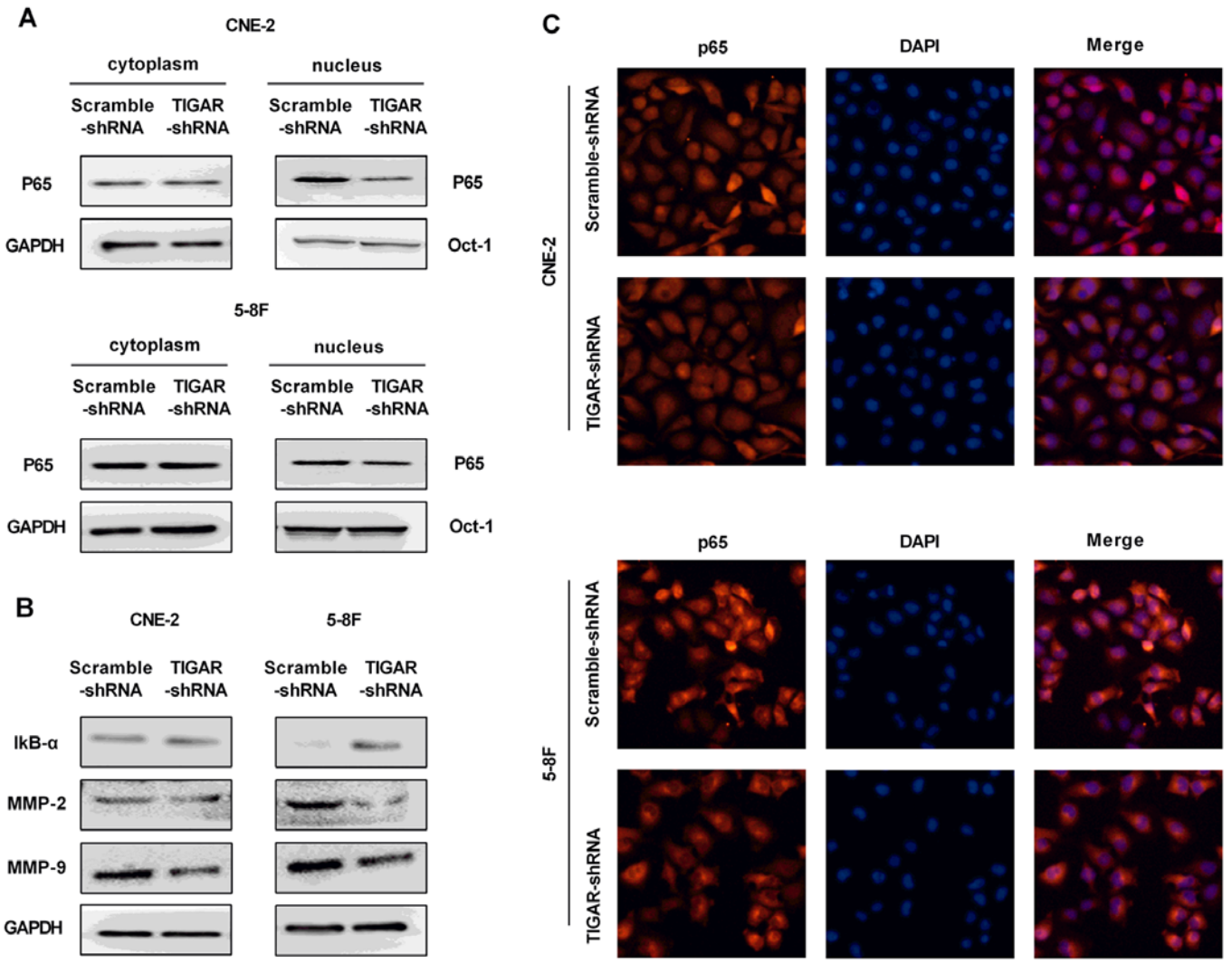

Figure 6. Knockdown of TIGAR inhibits the activity of NF-κB signaling pathway. (A) Western blot analysis of p65 in the cytoplasm and the nucleus. GAPDH and Oct-1 were used as loading control in cytoplasm and nucleus, respectively. (B) NF-κB pathway related gene expression is shown. (C) Representative microphotographs showing the nuclear translocation of p65. Nucleus was stained with DAPI. The original magnification was x200.

F-2,6-P2 levels and glycolytic flux (4,11,14). As PPP plays an important role in NAPDH production, knockdown of TIGAR results in decreased levels of NAPDH (15-17) and reduced glutathione (4,9,17), contributing to the accumulation of ROS (18). Through knockdown of TIGAR, our results confirmed the elevated ratio of GSH/GSSG and accumulation of ROS in NPC cells.

We further investigated the underlying mechanisms involved in NPC progress and we discovered a correlation between TIGAR and NF-κB pathway in NPC. NF-κB is a transcription factor composed of five subunits, including RelA (p65), RelB, cRel, NFKB1 (p50/p105) and NFKB2 (p52/p100) (19). In unstimulated cells, NF-κB binds to a class of inhibitory proteins called IκB (inhibitor of κB), which mask the nuclear localization signals (NLS) of NF-κB proteins and keeps them sequestered in an inactive state in the cytoplasm (20). Upon stimulation, IκB is phosphorylated by IκB kinase (IKK) and subsequently degraded, resulting in a rapid NF-κB translocation into the nucleus (21). Then, specific genes with NF-κB binding sites are activated, such as matrix metalloproteinase (MMPs) that degrade the extracellular matrix to facilitate cell invasion (22).

Numerous studies reported that NF-κB was constitutively active in many different types of human tumors, and exerted pro-tumorigenic functions (23). The oncogenic role of NF-κB in NPC was widely investigated in the past decade, revealing its function as a regulator of genes that control cell proliferation and cell survival, and protect the cell from apoptosis (24-28). Herein, we discovered a correlation between TIGAR and NF-κB pathway in NPC. Our results showed that knockdown of TIGAR contributed to NF-κB pathway inactivation in NPC cells, with an increased IκB-α expression, and an inhibited translocation of p65 into the nucleus, indicating an inhibited NF-κB pathway, thus supporting the role of TIGAR as a tumor promoter.

In the present study, we evaluated the effect of chemotherapeutics in combination with TIGAR depletion on apoptosis *in vitro*. Our results showed that TIGAR depletion can significantly promote the adriamycin-induced apoptosis. However, it is still unknown whether this effect can be obtained *in vivo*.

Radiation destroys genomic DNA to induce apoptosis (29). As a scavenger of intracellular ROS, TIGAR is capable of maintaining genomic DNA stability. Therefore, we assume that depletion of TIGAR may enhance the radiosensitivity of tumors. However, this aspect needs further clarification.

In conclusion, this study reported a higher expression of TIGAR in NPC tissues, compared with the adjacent normal epithelium. Knockdown of TIGAR by lentivirus-shRNA in NPC cells CNE-2 or 5-8F contributed to a reduction in cell growth and increased apoptotic rate. In addition, xenograft tumor models revealed the tumor promotor role of TIGAR. Furthermore, to our knowledge, this is the first report introducing the involvement of the NF-κB pathway in the TIGAR-inducing NPC tumorigenesis. The present study highlighted the oncogenic role of TIGAR in NPC tumorigenesis, underlining a potential role of TIGAR as a therapeutic target for cancer treatment.

Acknowledgements

This study was supported by grants from the National Natural Science Foundation (grant no. 81201784), Scientific Research Foundation of the Education Department of Sichuan Province (15ZA0163), the Union Project of Luzhou City and Sichuan Medical University (2013LZLY-J40), and The First Hospital of Sichuan Medical University Foundation (grant no. 201519).

References

1. Li XJ, Ong CK, Cao Y, Xiang YQ, Shao JY, Ooi A, Peng LX, Lu WH, Zhang Z, Petillo D, *et al*: Serglycin is a theranostic target in nasopharyngeal carcinoma that promotes metastasis. Cancer Res 71: 3162-3172, 2011.
2. Xiao WW, Huang SM, Han F, Wu SX, Lu LX, Lin CG, Deng XW, Lu TX, Cui NJ and Zhao C: Local control, survival, and late toxicities of locally advanced nasopharyngeal carcinoma treated by simultaneous modulated accelerated radiotherapy combined with cisplatin concurrent chemotherapy: Long-term results of a phase 2 study. Cancer 117: 1874-1883, 2011.
3. Lee AW, Lin JC and Ng WT: Current management of nasopharyngeal cancer. Semin Radiat Oncol 22: 233-244, 2012.
4. Bensaad K, Tsuruta A, Selak MA, Vidal MN, Nakano K, Bartrons R, Gottlieb E and Vousden KH: TIGAR, a p53-inducible regulator of glycolysis and apoptosis. Cell 126: 107-120, 2006.
5. Vousden KH and Ryan KM: p53 and metabolism. Nat Rev Cancer 9: 691-700, 2009.
6. Won KY, Lim SJ, Kim GY, Kim YW, Han SA, Song JY and Lee DK: Regulatory role of p53 in cancer metabolism via SCO2 and TIGAR in human breast cancer. Hum Pathol 43: 221-228, 2012.
7. Ye L, Zhao X, Lu J, Qian G, Zheng JC and Ge S: Knockdown of TIGAR by RNA interference induces apoptosis and autophagy in HepG2 hepatocellular carcinoma cells. Biochem Biophys Res Commun 437: 300-306, 2013.
8. Cheung EC, Athineos D, Lee P, Ridgway RA, Lambie W, Nixon C, Strathdee D, Blyth K, Sansom OJ and Vousden KH: TIGAR is required for efficient intestinal regeneration and tumorigenesis. Dev Cell 25: 463-477, 2013.
9. Wanka C, Steinbach JP and Rieger J: Tp53-induced glycolysis and apoptosis regulator (TIGAR) protects glioma cells from starvation-induced cell death by up-regulating respiration and improving cellular redox homeostasis. J Biol Chem 287: 33436-33446, 2012.
10. Sinha S, Ghildiyal R, Mehta VS and Sen E: ATM-NFκB axis-driven TIGAR regulates sensitivity of glioma cells to radiomimetics in the presence of TNFα. Cell Death Dis 4: e615, 2013.
11. Pena-Rico MA, Calvo-Vidal MN, Villalonga-Planells R, Martinez-Soler F, Gimenez-Bonafe P, Navarro-Sabate A, Tortosa A, Bartrons R and Manzano A.. TP53 induced glycolysis and apoptosis regulator (TIGAR) knockdown results in radiosensitization of glioma cells. Radiother Oncol 101: 132-139, 2011.
12. Wang L, Wei D, Huang S, Peng Z, Le X, Wu TT, *et al*. Transcription factor Sp1 expression is a significant predictor of survival in human gastric cancer. Clin Cancer Res 9: 6371-6380, 2003.
13. Somasundaram K and El-Deiry WS: Inhibition of p53-mediated transactivation and cell cycle arrest by E1A through its p300/CBP-interacting region. Oncogene 14: 1047-1057, 1997.
14. Kimata M, Matoba S, Iwai-Kanai E, Nakamura H, Hoshino A, Nakaoka M, Katamura M, Okawa Y, Mita Y, Okigaki M, *et al*: p53 and TIGAR regulate cardiac myocyte energy homeostasis under hypoxic stress. Am J Physiol Heart Circ Physiol 299: H1908-H1916, 2010.
15. Lui VW, Lau CP, Cheung CS, Ho K, Ng MH, Cheng SH, Hong B, Tsao SW, Tsang CM, Lei KI, *et al*: An RNA-directed nucleoside anti-metabolite, 1- (3-C-ethynyl-beta-d-ribo-pentofuranosyl) cytosine (ECyd), elicits antitumor effect via TP53-induced Glycolysis and Apoptosis Regulator (TIGAR) downregulation. Biochem Pharmacol 79: 1772-1780, 2010.
16. Lui VW, Wong EY, Ho K, Ng PK, Lau CP, Tsui SK, Tsang CM, Tsao SW, Cheng SH, Ng MH, *et al*: Inhibition of c-Met downregulates TIGAR expression and reduces NADPH production leading to cell death. Oncogene 30: 1127-1134, 2011.
17. Yin L, Kosugi M and Kufe D: Inhibition of the MUC1-C oncoprotein induces multiple myeloma cell death by down-regulating TIGAR expression and depleting NADPH. Blood 119: 810-816, 2012.
18. Bensaad K, Cheung EC and Vousden KH: Modulation of intracellular ROS levels by TIGAR controls autophagy. EMBO J 28: 3015-3026, 2009.
19. Napetschnig J and Wu H: Molecular basis of NF-κB signaling. Annu Rev Biophys 42: 443-468, 2013.
20. Jacobs MD and Harrison SC: Structure of an IkappaBalpha/NF-kappaB complex. Cell 95: 749-758, 1998.
21. Perkins ND and Gilmore TD: Good cop, bad cop: The different faces of NF-kappaB. Cell Death Differ 13: 759-772, 2006.
22. Karin M, Cao Y, Greten FR and Li ZW: NF-kappaB in cancer: From innocent bystander to major culprit. Nat Rev Cancer 2: 301-310, 2002.
23. Li F, Zhang J, Arfuso F, Chinnathambi A, Zayed ME, Alharbi SA, Kumar AP, Ahn KS and Sethi G: NF-κB in cancer therapy. Arch Toxicol 89: 711-731, 2015.
24. Ren Q, Sato H, Murono S, Furukawa M and Yoshizaki T: Epstein-Barr virus (EBV) latent membrane protein 1 induces interleukin-8 through the nuclear factor-kappa B signaling pathway in EBV-infected nasopharyngeal carcinoma cell line. Laryngoscope 114: 855-859, 2004.
25. Lo AK, Lo KW, Tsao SW, Wong HL, Hui JW, To KF, Hayward DS, Chui YL, Lau YL, Takada K, *et al*: Epstein-Barr virus infection alters cellular signal cascades in human nasopharyngeal epithelial cells. Neoplasia 8: 173-180, 2006.
26. Cheung AK, Ko JM, Lung HL, Chan KW, Stanbridge EJ, Zabarovsky E, Tokino T, Kashima L, Suzuki T, Kwong DL, *et al*: Cysteine-rich intestinal protein 2 (CRIP2) acts as a repressor of NF-kappaB-mediated proangiogenic cytokine transcription to suppress tumorigenesis and angiogenesis. Proc Natl Acad Sci USA 108: 8390-8395, 2011.
27. Sun W, Guo MM, Han P, Lin JZ, Liang FY, Tan GM, Li HB, Zeng M and Huang XM: Id-1 and the p65 subunit of NF-κB promote migration of nasopharyngeal carcinoma cells and are correlated with poor prognosis. Carcinogenesis 33: 810-817, 2012.
28. Kan R, Shuen WH, Lung HL, Cheung AK, Dai W, Kwong DL, Ng WT, Lee AW, Yau CC, Ngan RK, *et al*: NF-κB p65 subunit is modulated by latent transforming growth factor-β binding protein 2 (LTBP2) in nasopharyngeal carcinoma HONE1 and HK1 cells. PLoS One 10: e0127239, 2015.
29. Pawlik TM and Keyomarsi K: Role of cell cycle in mediating sensitivity to radiotherapy. Int J Radiat Oncol Biol Phys 59: 928-942, 2004.